J. Chem. Sci. (2020)132:127
https://doi.org/10.1007/s12039-020-01809-x

REVIEW ARTICLE

Heavy-atom tunneling in organic transformations

SHARMISTHA KARMAKAR and AYAN DATTA*
School of Chemical Sciences, Indian Association for the Cultivation of Science, 2A and 2B Raja S. C. Mullick Road, Jadavpur, Kolkata 700 032, India
E-mail: spad@iacs.res.in

MS received 11 February 2020; accepted 14 May 2020

Abstract. The pronounced effect of quantum mechanical tunneling in chemical reactions involving light atoms like hydrogen is well established. Recent studies have found that tunneling can also play a significant role for common organic transformations, where if the participating atom is carbon/nitrogen, etc. For these cases, various reaction parameters like reaction barrier, barrier width and temperature play a crucial role in determining the efficiency of tunneling. In this review, we have focused on all those organic transformations where the influential role of tunneling has been documented either computationally or experimentally.

Keywords. Organic transformations; heavy-atom tunneling; reaction kinetics; kinetic isotope effect.

1. Introduction

Quantum mechanical tunneling (QMT) is a fundamental physical phenomenon that is being realized as a key factor in many chemical and biological transformations. Over the last 80 years, the tunneling effects have been realized predominantly for H-atom mediated reactions like H–transfer, C–H insertion. Anomalously, large kinetic isotope effect (KIE) serve as an experimental signature for tunneling.[1–6] Since the tunneling probability depends strongly on the mass of moving particle, the effects of tunneling are subtle for reactions involving heavy atoms. In the early 1900's, it was believed that particle heavier than helium do not tunnel, as Bell mentioned in his 1933 paper that "It must, however, be emphasized that all atoms heavier than helium behave, practically speaking, classically."[7]

The major experimental evidence for heavy-atom tunneling was first reported by Buchwalter and Closs in 1975. They observed that the decay rates of triplet cyclopentane-1,3-diyl (1) to bicycle [2.1.0] are temperature-independent from 1.3 K to 20 K in matrix environment.[8] The occurrence of the ring closure reaction at cryogenic temperature is a typical signature of heavy-atom tunneling through a low barrier. In 1982, another experimental finding indicated the involvement of carbon tunneling in automerization of cyclobutadiene at cryogenic temperatures.[9] In the very next year, Carpenter interpreted the experimental results published in 1982 paper, taking into account the tunneling effects by theoretical modeling, and he also mentioned that under experimental reaction condition, at least 97% of the reaction occurs by tunneling below 0°C, which results in negative entropy factor.[10] This is one of the classic examples of heavy-atom tunneling.

Slowly, the idea of "heavy-atom tunneling can affect the reaction kinetics" gained momentum and more theoretical supports for heavy-atom tunneling are reported; however, its experimental manifestations are less obvious.[11–13] The detection of heavy-atom tunneling is rather difficult. Reactions occurring at cryogenic temperature are the most common example of reactions involving significant contribution from heavy-atom tunneling as at this temperature, there is very less thermal energy to cross the barrier. For reactions that are carried out at non-cryogenic temperatures; primary and secondary kinetic isotope effect study act as an experimental indicator of heavy-atom tunneling.[5] Nevertheless, accurate theoretical calculations can always be used to study the contribution of tunneling in particular transformations. In the last decade, several other reactions where heavy-atom tunneling have been documented are ring closure of cyclopentane-1,3-diyl[8,14] and cyclobutane-1,3-diyl,[15] rearrangement of cyclopropyl carbenes,[16] Myers–Saito cyclization of annulene,[17] ring opening of the cyclopropylcarbinyl

*For correspondence

Published online: 12 September 2020

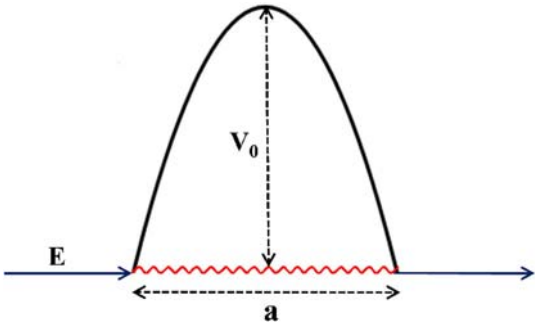

Figure 1. Tunneling across a parabolic barrier of width, a, and height V_0, at an energy E.

radical,[18,19] rearrangement of semibullvalene,[20] Bergman cyclization of a 10-membered-ring enediyne[21] and ring expansion of noradamantyl carbenes and their analogs.[22,23] A salient feature of the mentioned list of reactions is a rather a low reaction barrier accompanied with a small displacement of carbon atoms from reactant to product.

We have subdivided this chapter into three parts. In the first two sections, we discuss about what is heavy-atom tunneling and how is it affected by the reaction parameters followed by its signature in every-day organic reactions. In the last section, we have discussed about those reactions which have been shown experimentally or predicted to involve significant heavy-atom tunneling in the course of reaction. Lastly, we conclude that at presents, heavy-atom tunneling is a well-established phenomenon occurring in a variety of chemical transformations.

2. Variation of tunneling probability with various reaction parameters

This section describes the dependency of tunneling probability (T) with particle mass, width of the barrier and barrier height for a parabolic barrier. The potential energy surface of a chemical reaction can be approximately described as parabolic function to a certain extent. The probability of tunneling (T) for an inverted parabolic potential following Jeffreys–Wenzel–Kramers–Brillouin (JWKB) approximation can be given by[12]

$$T(E) = \frac{1}{1 + e^{\pi^2 a\sqrt{2m(V_0 - E)}/h}}, \quad (1)$$

where a is the barrier width, m is particle mass, V_0 represents the height of the barrier and E corresponds to the energy of the particle (see Figure 1). Thus, the tunneling probability is inversely proportional to the exponential of the square root of the barrier height, exponential of the square root of the particle mass and exponential of the barrier width.

We have performed model calculations to get a quantitative estimate of tunneling probability for a normal organic reaction. We have tried to figure out how variation of different reaction parameters like, barrier height and particle mass, and barrier width affect the tunneling probability.

As quantum mechanical tunneling (QMT) is more evident for H-mediated reactions, we have calculated the probability of a H-atom tunneling across a parabolic barrier of 1 Å thickness with a barrier height of $\Delta E^{\neq}$ = 10 kcal/mol. The probability of H-tunneling

Sharmistha Karmakar obtained her Ph.D. in 2018 from Indian Association for the Cultivation of Science, India for computational chemistry, working on examples of quantum mechanical tunnelling in organic and organometallic chemistry under the supervision of Prof. Ayan Datta. She is currently a postdoctoral researcher at University of Maryland, USA. Her current research focuses on the interactions of lipid bilayer with peripheral membrane proteins using molecular dynamics simulations.

Ayan Datta obtained his Ph.D. degree in 2007 from the Jawaharlal Nehru Centre for Advanced Scientific Research. After postdoctoral work in University of North Texas he joined the Indian Institute of Science Education and Research Thiruvananthapuram. He moved to Indian Association for the Cultivation of Science in 2012 where he is a Professor. His research interests are in computational materials science and applied theoretical chemistry. He uses simple models of bonding and reactivity to derive a qualitative understanding of behaviour of matter at various length and time-scales.

following equation 1 was calculated to be $T(E) = 1.6 \times 10^{-10}$ and the rate of tunneling (calculated assuming the H atom is vibrating with a typical frequency of 1000 cm^{-1}) was found to be 4.6×10^3 s^{-1}. Thus, our calculations indicate that for a typical organic reaction with $\Delta E^{\neq} = 10$ kcal/mol and $a \approx 1$ Å, involving appreciable H-atom motion in the rate-determining step, tunneling contributes significantly to the overall reaction rate, whereas, the probability of tunneling for a C-atom was found to be negligible with similar reaction parameters ($T(E) = 1.6 \times 10^{-34}$). Hence, a 10^{24}-fold decrease in the tunneling rate (3.3×10^{-21} s^{-1}) was attributed to 12-times greater tunneling mass of carbon than hydrogen.

Further, we tried to find out the right combination of barrier height and barrier width, which is crucial for getting significant tunneling contributions for reactions involving heavy atom motions. Thus, reducing the barrier height to half, i.e. $\Delta E^{\neq} = 5$ kcal/mol, increases the probability of tunneling by 10^9-fold for a C-atom across 1Å parabolic barrier and the tunneling rate was calculated as 2.9×10^{-11} s^{-1} (assuming the C-atom is vibrating with a typical C–C frequency of 1000 cm^{-1}).

On the other hand, reducing the barrier width to 0.5 Å has a 10^8 times greater impact on the tunneling probability than the reduction of barrier height to similar extent for a C-atom. Thus, the tunneling rate for a C-atom tunneling through a parabolic barrier of 0.5 Å thickness and 10 kcal/mol height was calculated to be 3.1×10^{-4} s^{-1}. Nevertheless, when both the barrier height and barrier width are reduced to values ($\Delta E^{\neq} = 5$ kcal/mol and $a \approx 0.5$ Å) half of their initial values, the tunneling rate for a C-atom was found to be 30.9 s^{-1} which indicates appreciable heavy-atom tunneling contribution to the overall rate. Therefore, heavy-atom tunneling is important for those organic reactions which have a low activation barrier along the narrow barrier.

The most popular and efficient kinetic model used for large systems is variational transition state theory with multidimensional tunneling (VTST/MT) correction developed by Truhlar and coworkers.[24] It provides reaction rate with reasonable accuracy, taking into account the recrossing effect by variational optimization of the dividing surface and tunneling correction through semi-classical treatment. Canonical variational transition state theory (CVT) is one of the useful variation of VTST which has been used extensively for various organic reactions, and the tunneling corrections are incorporated by multidimensional tunneling methods, such as zero-curvature tunneling (ZCT) approximation, small-curvature tunneling (SCT) approximation and large-curvature tunneling (LCT) approximation, among which SCT is the most versatile method in terms of both accuracy and computational cost.[24]

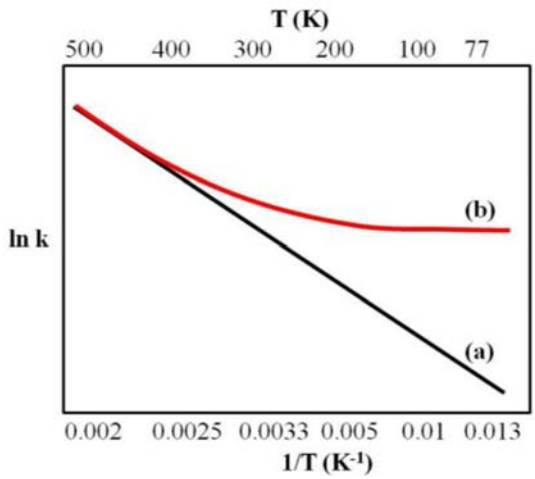

Figure 2. A typical Arrhenius plot for a reaction showing (a) linear plot for a classical over the top of barrier process and (b) with effects of QMT (Reprinted with permission from ref 26. Copyright © 2016 Elsevier Ltd.)

3. Footprints of heavy-atom tunneling in organic reactions

As the probability of tunneling is highly sensitive to the mass of moving particle, the tunneling effects become subtle for reactions involving heavy atoms compared to reactions involving hydrogen atom motion. (As the probability of tunneling is inversely proportional to the mass of tunneling particle, the effect of tunneling gets diminished with increasing mass). Hence, the tunneling effects are subtle for heavy atom reactions. Therefore, experimental detection of heavy-atom tunneling becomes less obvious, especially at room temperature. Despite these facts, there are some specific signatures which clearly indicate the participation of heavy-atom tunneling in chemical reactions. We will discuss them in systematic order.

3.1 *Temperature independence of reaction rate*

The study of temperature (T) dependence of reaction rate provides valuable information about the effects of tunneling in a chemical reaction. For a typical classical organic reaction, the reaction rate shows linear dependency with temperature following Arrhenius

equation. However, for reactions with significant tunneling corrections, the actual rate becomes independent of temperature as can be seen from the flat region of red curve in Figure 2. This observation can solely be described by tunneling effects. At very low T, all the molecules reside at their vibrational ground state ($v = 0$) and do not possess enough energy to cross the barrier. The only thing that they can do is to tunnel from their lowest vibrational quantum levels without thermal activation. Under this circumstance, the reaction rate is solely governed by the efficiency of tunneling of the concerned part of the reacting molecule, and as a consequence, the rate becomes independent of T.[25]

As temperature rises, higher vibrational levels are populated and tunneling through narrower barrier from the excited vibrational levels becomes more facile leading to enhanced rate. Therefore, at intermediate temperature range, thermally activated tunneling along with classical over-the-barrier process makes Arrhenius plot moderately curved. Thus, observation of a curved Arrhenius plot or temperature-independent rate constant for reactions involving heavy atom motions act as strong signature for heavy-atom tunneling.[26]

3.2 *Reactions occurring at cryogenic temperature*

Reactions occurring at cryogenic temperature serve as the most common evidence of heavy-atom tunneling. QMT usually makes a chemical reaction faster from the classical over–the–barrier process and the effect of tunneling is more spectacular at cryogenic temperatures (T<77 K). At extremely low temperatures, reactions with very small activation barriers ($\sim$1 kcal/mol) are also forbidden classically as it requires 114 years to reach half–life for a unimolecular transformation with E_a = 1 kcal/mol at 10 K. However, quantum mechanical tunneling increases the reaction rate by several order of magnitudes from its classically predicted value and allows the reaction to occur with a measurable rate constant at this low T. Many reactive intermediates are known to undergo various types of chemical transformations with appreciable rate constants at extremely low T, exclusively by tunneling through a considerable energy barrier.[27]

3.3 *Large kinetic isotope effects*

Because of the $(\text{mass})^{1/2}$ dependence of the tunneling probability, isotopic substitution affects the reaction rate more dramatically than predicted, based on zero–point vibrational energy differences. The greater tunneling efficiency of the lighter particle compared to the heavier one is the primary reason for these anomalously large isotope effects. As the de Broglie wavelength varies inversely with mass of the moving particle, the lighter particle possesses longer wavelength which facilitates the barrier penetration. On the other hand, the heavier isotope having lower vibrational zero-point energy sits in deeper region of the energy well and hence, experiences an effectively wider barrier. These two effects act together to retard the tunneling efficiency of the heavier particle selectively and deviate the Arrhenius plots of KIE from linearity. The observed kinetic isotope effect is given by:[25]

$$k_A^L/k_A^H = \left(k_s^L/k_s^H\right) \times \left(Q^L/Q^H\right),$$

where $\left(k_s^L/k_s^H\right)$s the semi-classical isotope effect, L and H symbolize light and heavy particle, respectively.

As the ratio of Q^L/Q^H is always greater than unity, the value of $k_A^L/k_A^H\left(k_s^L/k_s^H\right)$ (equality holds for systems where both isotopes have similar tunneling correction). Hence, the effect of heavy-atom tunneling on the $^{12}C/^{13}C$ KIE is to increase the value of isotope effect above the one predicted by the semi-classical treatment. Therefore, observation of nonlinear Arrhenius plot of KIE or large ^{13}C KIE is another footprint of heavy-atom tunneling.[25]

4. Examples of organic reactions involving heavy-atom tunneling

In this section, we have listed all those reactions which have been shown to involve significant heavy-atom tunneling either experimentally or computationally. The first two sections comprise few early examples of heavy-atom tunneling which have been observed experimentally. In the following section, we focus on several other types of reaction where tunneling by heavy atom was found to play a key role. All these examples show the importance of calculations to determine the effect of heavy-atom tunneling.

4.1 *Carbon tunneling in the ring closure reactions of triplet 1,3-diradicals*

In 1975, Buchwalter and Closs studied the decay kinetics of triplet 1,3-cyclopentadiyl **1** to **2** by electron spin resonance (ESR) spectra in matrix isolation at

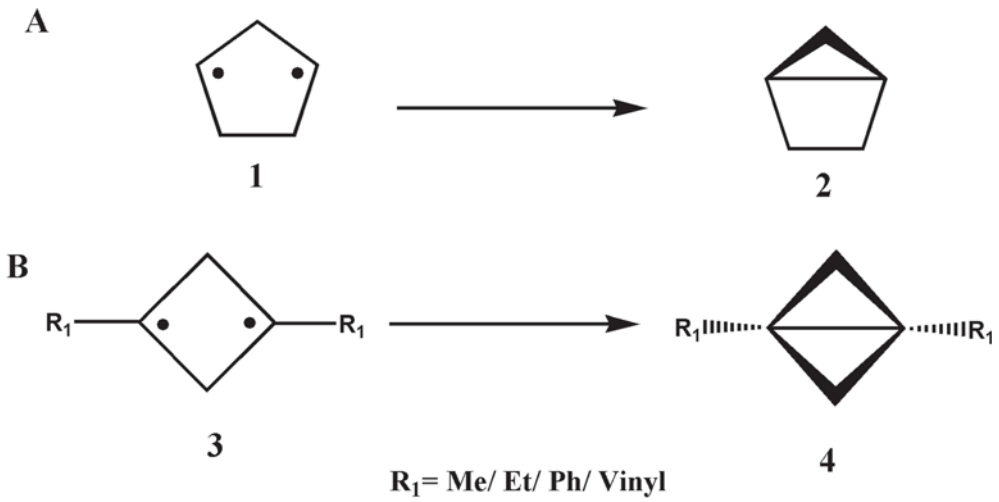

Scheme 1. The ring closer reaction of triplet diradicals (A) cyclopentane-1,3-diyl (**1**) to bicyclo[2.1.0]pentane (**2**), (B) cyclobutane-1,3-diyl (**3**) to bicyclo[1.1.0]butane (**4**).

cryogenic temperatures (Scheme 1). They observed that the decay kinetics of **1** follows non-exponential behavior over the studied temperature range irrespective of the matrix element. Additionally, it was also found that the reaction rate is temperature-independent between 1.3 to 20 K. Thus, the authors suggested that the reaction occurs by heavy-atom tunneling through a barrier of 2.3 ± 0.2 kcal/mol because such kinetics behavior is a typical characteristic of QMT.[8]

Later, in 1989, Sponsler *et al.* performed detailed experimental studies on the ring closure reaction of analogous triplet diradicals, namely substituted 1,3-cyclobutanediyls **3** under matrix isolation. With strong radical-stabilizing substituents, like vinyl and phenyl, **3** was found to be stable up to 20 K and above, the reaction occurred by thermal activation following Arrhenius behavior. While for the other substituents, e.g., methyl and ethyl, the less stabilized radicals undergo the ring closure even at 4 K. The decay rates were found to be temperature insensitive, indicating a tunneling mechanism for the **3**→**4** transformation. The contrasting behavior of the stabilized radicals vs. the localized ones was explained in terms of widening of the reaction barrier for the radical-stabilizing groups which subsequently suppress the tunneling.[14]

4.2 *Tunneling in the isomerization of cyclobutadiene-d_2*

In 1982, Whitman and Carpenter reported a surprising finding while studying the temperature and concentration dependence of the trapping reaction of cyclobutadiene (CDB)-d_2 in CH_2Cl_2. They measured the temperature dependence of the relative rates and compared the activation parameters for two competitive reactions, namely automerization of CBD-1,4-d_2 (**5**) to CBD-1,2-d_2 (**6**) and trapping of **5** by Diels–Alder cycloaddition reaction (Scheme 2). It was found that the entropy of activation ($\Delta S^{\#}$) for the automerization reaction of CBD is only 8 eu more positive than the corresponding cycloaddition reaction. However, for a typical bimolecular reaction like Diels-Alder cycloaddition, the $\Delta S^{\#}$ value lies in the range from −25 to −40 eu, while the same for a unimolecular reaction is expected to be $\Delta S^{\#} \approx 0$. Thus, the observation of very low value of $\Delta S^{\#}$ for the

Scheme 2. The automerization of CBD-1,4-d_2 (**5**) to CBD-1,2-d_2 (**6**).

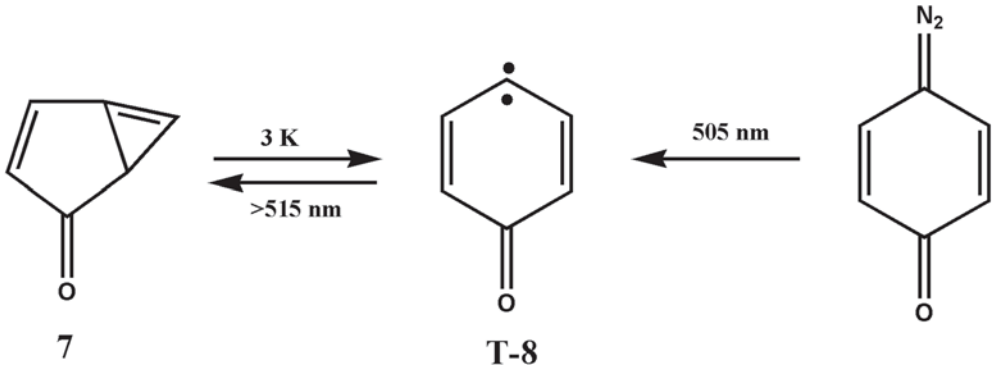

Scheme 3. The ring opening rearrangement of a strained cyclopropene **7**.

automerization reaction is highly surprising and the authors could not explain this result.[9]

In the very next year, Carpenter explained these unusual findings by invoking the concept of heavy-atom tunneling.[10] They estimated the barrier height and width for the **5→6** reaction to be 10.8 kcal/mol and 0.18 Å, respectively. The tunneling rates were calculated by Bell's formula through a truncated parabolic potential, and the reaction rates were found to be 8.08×10^4 s^{-1} and 4.65×10^5 s^{-1} at −50 and −10°C, respectively. The author concluded that 97% of the automerization reaction of CBD occurred due to heavy-atom tunneling below 0°C. The tunneling activation parameters were calculated to be $\Delta H^{\#} = 4.6$ kcal/mol and $\Delta S^{\#} = -15$ eu which suggests that the tunneling occurs from vibrational excited states. Nevertheless, the author concluded that unexpectedly small Arrhenius A factor associated with large negative entropy of activation for a unimolecular reaction is a clear indication of QMT.

4.3 *Tunneling by carbon in the ring opening of a strained cyclopropene*

The ring opening of **7** to **T-8** at cryogenic temperatures comprises another interesting example of heavy-atom tunneling (Scheme 3). The cyclopropene **7** is produced by the irradiation of the triplet carbene T**-8** at 10 K while the **T-8** is formed by the photolysis of its corresponding diazo compound in matrix isolation. On standing, the **7** rearranges to **T-8** at temperatures as low as 3 K, irrespective of the matrix element, showing a non-linear Arrhenius plot with temperature independent rate constants below 20 K.[28] The temperature-independent nature of the Arrhenius plots is a clear indication of tunneling from the lowest vibrational state, implying zero activation energy below 20 K whereas, thermally activated tunneling takes place above 25 K. In spite of strong matrix effect, the measured rate was found to be in the order of 10^{-6} s^{-1}.[28]

As the reactant **7** and the product **T-8** possess singlet and triplet ground states respectively, intersystem crossing (ISC) must occur to accomplish the rearrangement. However, this step could not be detect in experiment. Detailed theoretical calculations were carried out to establish the mechanism for the interconversion at (8/8) CASSCF and CASPT2 levels. Theoretical calculations have identified the triplet carbene, **T-8** as well as its lowest open shell singlet state, **S-8** which has energy lower than **7**. It was proposed that the **7** rearranges to **S-8** via QMT, followed by **S-8** to **T-8** interconversion by ISC. The barrier height and reaction energy at the more effective CASPT2 level was calculated to be 8 kcal/mol and −4 kcal/mol respectively. Computations of reaction rates at CASPT2/cc-PVDZ level shows that the reaction is temperature independent below 50 K and the calculated SCT rate constant was $k = 2.4 \times 10^{-6}$ s^{-1} which is very close to the experimentally measured Ar matrix, thus, confirming the tunneling mechanism for this reaction.[28]

4.4 *Heavy-atom tunneling in carbene ring expansion*

The 1,2-shifts are most common type of rearrangement in carbene where the β-substituents (e.g. –H, –R, –Ar, –OR, –SR, –F and –Cl) migrate to the carbene center resulting in the formation of a double bond.[29] The reactivity of the carbene strongly varies depending on its substituents and chemical structure. The alkyl group migration is favored in cyclic strained carbene. The contribution of heavy-atom tunneling in 1,2-C migration for various carbene systems was

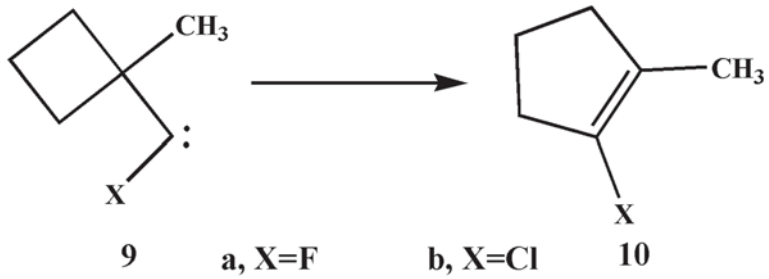

Scheme 4. Ring expansion of 1-methylcyclobutylhalocarbenes (**9**) to1-halocyclopentenes (**10**).

investigated by several experimental and theoretical groups which we will focus successively.

4.4a *Ring expansion of 1-methylcyclobutylhalocarbenes to 1-halocyclopentenes*: In 2003, Sheridan studied the decay kinetics of ring expansion rearrangement of cyclobutylhalocarbenes (**9**) to 1-halocyclopentenes (**10**) at very low temperatures (8–25 K) in matrix isolation (Scheme 4).[30] The carbenes were generated by photolysis of their corresponding alkylhalodiazirines and can be identified by their characteristic IR band at low temperatures. However, upon irradiation of chlorodiazirine at 8 K in N_2 matrix, no signal of chlorocarbene (**9b)** was observed in the IR spectra because of its very high reactivity. Stronger ∏-donor ability of F compared to Cl stabilizes the fluorocarbene (**9a)** more effectively than the **9b**, as a result **9a** can be detected by IR spectra at 8 K. The rate constant for the ring expansion reaction of **9a→10a** was measured to be 4×10^{-6} s^{-1} at 8 K in N_2 matrix. The rearrangement of **9a** becomes 10 times more facile in Ar matrix with a rate constant of 4×10^{-5} s^{-1} at 8 K. When the temperature is doubled to 16 K, the rate of disappearance of **9a** in Ar matrix increases only by a factor of two ($k = 9 \times 10^{-5}$ s^{-1} at 16 K for **9a→10a)**. Such negligible increment in the rate constants upon increasing the temperature from 8 K to 24 K is inconsistent with thermally activated processes and indicates the presence of a strong carbon atom tunneling for such transformation.

To validate the experimental findings, detailed theoretical calculations were performed and the tunneling effects were included by SCT approximation. The calculated barriers for the rearrangement of **9a** and **9b** were found to be 6.5 and 3.1 kcal/mol respectively, which are too high to be surmounted thermally by the reactant molecules at experimental temperatures. The tunneling corrected rate constants for the rearrangement reaction of **9a** and **9b** were found to be 9.1×10^{-6} s^{-1} and 1.4×10^{4} s^{-1} respectively, at 8 K. The corresponding half-lives ($t_{1/2}$) are 10^{-4} s and 21 h for chlorocarbene **9b** and fluorocarbene **9a**; respectively. Such ultra-short calculated half-life for chlorocarbene **9b** is the reason for its failure of detection in IR spectra by the authors. Also, the SCT calculated rate for fluorocarbene **9a** shows an excellent agreement with the measured rate at 8 K in Ar matrix. The vanishing of activation energy at low temperatures for **9a** is a clear indication of carbon tunneling from the vibrational ground state without any thermal activation. Thus, the very small increment of rate constant in the temperature range of 8–25 K was attributed to the matrix softening effect. Therefore, the calculations confirm the presence of heavy-atom tunneling in the ring expansion rearrangement of **9a→10a** as without tunneling, the calculated rate constants were lower by a factor of 10^{52} for **9b** and 10^{152} for **9a** at 8 K which clearly omits any occurrence of reaction by thermal activation at such low temperatures.[30]

4.4b *Ring expansion of noradamantylcarbenes, adamantylcarbene and bisnoradamantylcarbenes*: Another interesting experimental observation of C-atom tunneling in carbene rearrangement came out in 2004 by Moss *et al.*[23] They reported that the ring expansion of the singlet noradamantylchlorocarbene (**11c**) to 2-chloroadamantene (**12c**) occurs by C-tunneling through the barrier at 9 K in N_2 matrix (Scheme 5). They prepared the chlorocarbene (**11c**) by irradiation of noradamantylchlorodiazirine at 8 K in N_2 matrix and **11c** was sufficiently stable to study its decay kinetics at cryogenic temperatures. Further, irradiation of the matrix isolated **11c** and readily rearranged it to **12c** within 6 h. Surprisingly, when the matrix-isolated chlorocarbenes, **11c** were kept in dark, the conversion did not stop, it still continued to yield **12c** at 9 K in N_2 matrix, and the product was identified by its characteristics of the IR spectra. The rate constant for this transformation (**11c→12c**) was measured to be

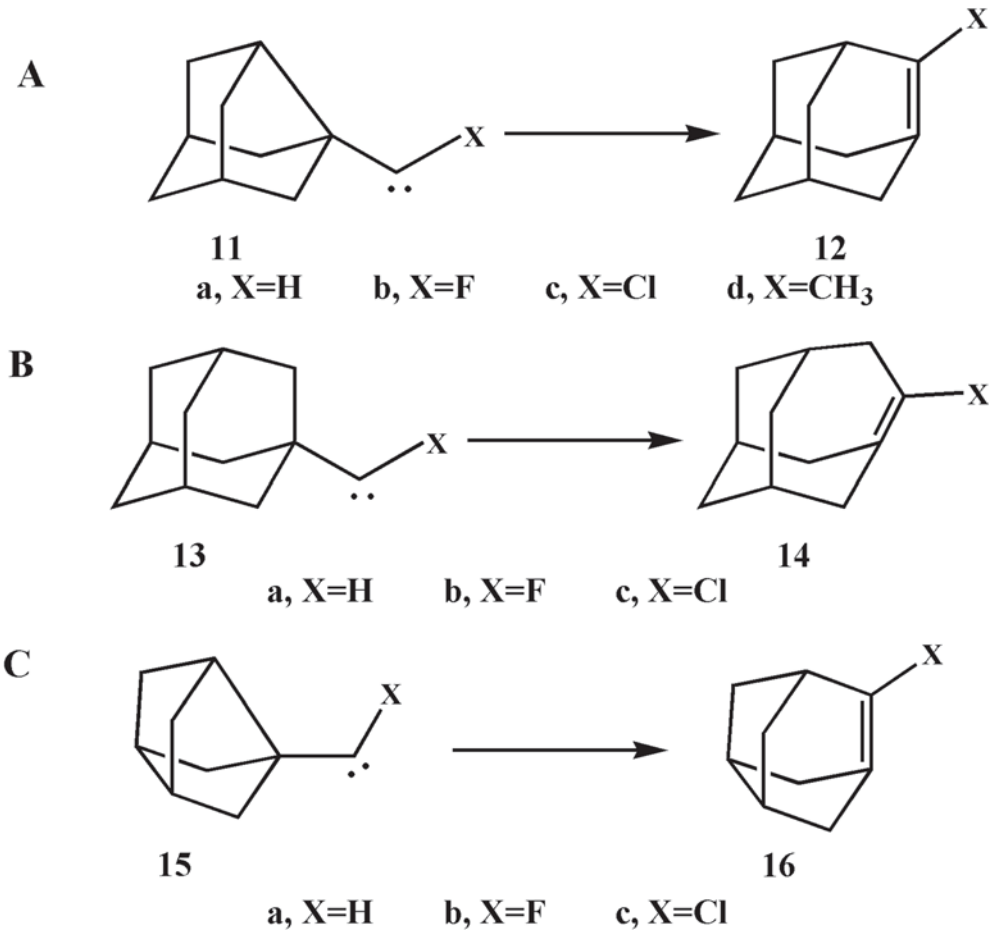

Scheme 5. Ring expansion of (A) noradamantylcarbenes (**11**) to adamantenes (**12**), (B) adamantylcarbene (**13**) to homoadamantene (**14**) and (C) bisnoradamantylcarbenes (**15**) to noradamantenes (**16**).

2.3×10^{-7} s^{-1} at 9 K in N_2 matrix. The barrier for this rearrangement reaction, **11c→12c**, was calculated to be 5.3 kcal/mol at the B3LYP/6-31G(d) level. Later, SCT rate constant calculations at the same level predicted the rate constant to be $k = 3.7 \times 10^{-7}$ s^{-1} at 9 K, which is within a factor of two of the experimental value and $\sim 10^{111}$ times faster than the classical over the barrier process at the same temperature. The barrier width for this rearrangement, **11c→12c**, was also found to be narrow; the maximum displacement of the carbenic center was only 0.44 Å. Thus, all these findings and similarity of decay kinetics of **11c** with **9a** ensure the fact that the rearrangement of **11c** to **12c** proceeds by C-atom tunneling at cryogenic temperatures.

Following the experimental observation of heavy-atom tunneling in noradamantylchlorocarbene (**11c**), Kozuch carried out a detailed study for analogous carbenes to find out the right combination of reactivity which can lead to experimentally observable lifetimes for the ring expansion process by C-tunneling at cryogenic temperatures.[22] The reactivity of the carbene is purely governed by the substituent X atom and the tension of the C_α–C_β bond. While halogen substitutions stabilize the carbene by p→p electron donation, the H-substitution makes it highly reactive and the stabilizing power of the X atom follows the order: F > Cl > H. On the other hand, the increasing strain in the neighboring C_α–C_β bond makes the ring expansion process more facile, indicating a shorter lifetime for the following carbene. To gain a deeper insight, Kozuch carried out a detailed rate constant calculation with SCT tunneling correction for the ring expansion of noradamantylcarbenes (**11**), adamantylcarbene (**13**) and bisnoradamantylcarbenes (**15**) with varying substituents (F or Cl or H). As can be seen from Scheme 5, the strain in the C_α–C_β bond is maximum for bisnoradamantylcarbenes (**15**) followed by noradamantylcarbenes (**11**) and adamantylcarbene (**13**) and subsequent barrier ($\Delta E^{\#}$) calculations also shows similar trend with **15** < **11** < **13**. They predicted that the carbenes **13b**, **13c** and **11b** will not produce any rearrangement products in measurable time at 10 K because of very high barrier for heavy-atom

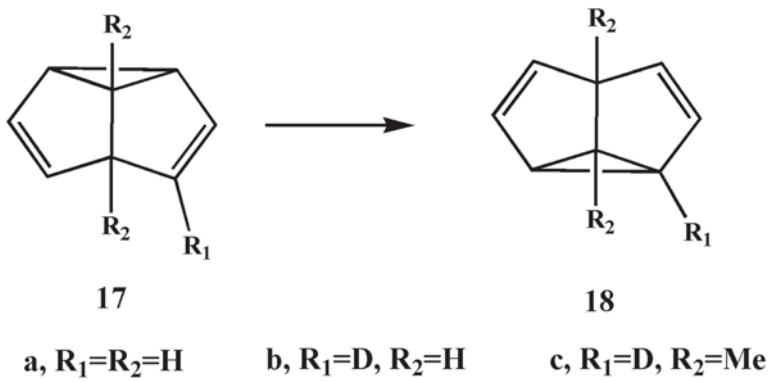

Scheme 6. The automerization of semibullvalene (**17a**) and its derivatives (**17b** and **17c**).

tunneling. While very low or nonexistent barriers for **11a**, **15a** and **15c** make the ring expansion process extremely facile, resulting in the detection of these carbenes and subsequent rate measurement impossible at cryogenic temperatures. Finally, according to their prediction, noradamantylchlorocarbene (**11c**), bisnoradamantylfluorocarbene (**15b**), and unsubstituted adamantylcarbene (**13a**) are the three experimentally observable systems, and C-tunneling from the lowest vibrational state makes these reactions feasible to observe experimentally even at 10 K.

4.5 *Heavy-atom tunneling in pericyclic reactions*

4.5a *Carbon tunneling in the automerization of semibullvalene and its derivatives*: Semibullvalene (**17a**) is known to undergo degenerate Cope rearrangement across a low energy barrier ($\Delta H^{\#}$) of 5.0 ± 0.2 kcal/mol (Scheme 6).[31] Along with low enthalpic barrier, the barrier also appears to be narrow, and the calculated change in C–C bond distances on breaking and forming cyclopropane ring bond in **17a** is 0.75 Å. Both the low-reaction barrier and narrowness of the barrier make this rearrangement reaction an ideal candidate to observe carbon tunneling at cryogenic temperatures. Detailed theoretical calculations including tunneling correction at SCT level by Zhang *et al.* predicted that the rates of the transformation (**17a→18a**) become temperature independent below 40 K, indicating carbon tunneling from the lowest vibrational state.[20] The half-time for the degenerate cope rearrangement of **17a** was calculated to be ~8 min at 40 K. The authors also proposed an experimental procedure to validate their theoretical prediction of carbon tunneling at cryogenic temperature for semibullvalene derivatives. Substitution of one H-atom at either at positions 2 or 4 of semibullvalene by D, makes the rearrangement reaction (**17→18b**) non-degenerate with a ΔG of −0.17 kcal/mol. For semibullvalene-d_1, isomer with D attached to the cyclopropyl ring carbon (**18b**) has a lower energy than the one where D is attached to the double-bonded carbon because of higher bending frequency of the C(sp^3)-H compared to C(sp^2)-H, which makes the zero-point energy lower in **18b** than in **17b**. The small difference in free energy correspond to an equilibrium constant of K = 1.25 at 300 K which increases to K = 5260 at 10 K. Therefore, rapidly converting equilibrium mixture of **17b** and **18b** at room temperature will generate a mixture that is far from equilibrium following a ratio of **18b**:**17b** = 5260:1 at cryogenic temperatures. Since the rearrangement reaction of **17b** possesses a barrier of ~5.0 kcal/mol, the predicted equilibrium population at cryogenic temperatures will only be achieved if the reaction occurs by tunneling. The rate of the Cope rearrangement can be measured by following the rate of disappearance of the higher energy isomer (**17b**) to the lower energy one (**18b**) at cryogenic temperatures.

Later in 2017, Schleif *et al.* confirmed the computational prediction of Zhang *et al.* by performing experiments on monodeuterated 1,5-dimethylsemibullvalene (**17c**) isotopomers using IR spectroscopy in matrix isolation.[32] They deposited a room temperature equilibrium mixture of 1,5-dimethylsemibullvalene-2(4)-d_1 isotopomers with a excess of neon on a CsI window at 3 K. As the two isotopomers possess its own characteristic IR peaks in the mid-IR region, the kinetics of the Cope rearrangement (**17c→18c**) was measured by following the changes in the IR intensities in that particular region. After keeping the matrix in dark for several hours, they found a decrease in the intensities of the IR peaks of the less stable isotopomer (**17c**) while the other one of **18c** increases. The

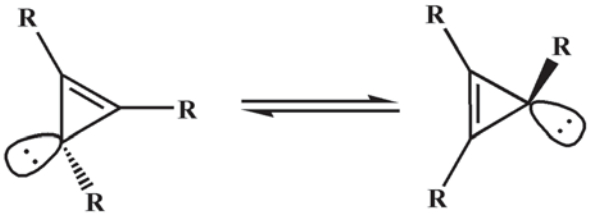

24a, R=H b, R=CN c, R=CH_3 d, R=F e, R=Ph

Scheme 7. The automerization of cyclopropenyl anion (**24a**) and its derivatives (**24b–24e**).

observation clearly demonstrates the occurrence of the Cope rearrangement of **17c→18c** at such low temperature of 3 K. As the barrier for this transformation (**17c→18c**) is significantly high (4.8 kcal/mol) to proceed by thermal activation below 10 K, the authors concluded that the Cope rearrangement occurs by heavy-atom tunneling below 10 K with a reaction rate in the order of 10^{-4} s^{-1}. Furthermore, they also studied the temperature dependence of the reaction rate and found that the rate is increasing only by a small factor in the temperature range of 3–30 K which is obvious for reactions governing by tunneling.

4.5b *Heavy-atom tunneling in the automerization of pentalene and other antiaromatic molecules*: Similar to cyclobutadiene (CBD), Kozuch has studied the role of heavy-atom tunneling in the automerization reactions of pentalene (PL, **19**), acepentalene (APL, **20**) and heptalene (HL, **21**) (Scheme 7).[33] All these molecules are antiaromatic in nature with 4nΠ electrons and possess C–C bonds with alternating bond lengths. Despite of structural similarities with CBD, presence of C–C bonds across the antiaromatic annulene rings make their electronic structures significantly different from that of CBD. Unlike CBD, the cross-ring bond between the bridgehead carbons in **19**, **20** and **21** lift the degeneracy of the HOMO and LUMO through the interaction of the 2p AOs on these carbons. Therefore, the automerization reactions in these molecules do not involve HOMO-LUMO crossing owing to significantly large HOMO-LUMO gaps and the author suggested that single-configuration wave-function will be sufficient to describe the systems.

The reaction rate constant calculations for these systems predicted that the pentalene (PL) can undergo facile Π-bond shifting reaction via tunneling of the ring carbons from vibrational ground state even at 10 K with a transient half-life of 3×10^{-9} s whereas the tunneling corrected rate constants for the automerization of HL and APL are $k = 1.2 \times 10^{-38}$ s^{-1} and $k = 1.2 \times 10^{-9}$ s^{-1} respectively at 10 K. Such small computed rate constants indicate that the double bonds in these molecules would be frozen at this temperature. The difference in tunneling reactivity between **19** on one hand, and **20** and **21** on the other was explained in terms of planarity of the equilibrium structures. Both the **20** and **21** possess a puckered non-planar geometry while the **19** comprises a planar equilibrium structure. Therefore, in order to follow the automerization pathway, the **20** and **21** must undergo some degree of planarization to reach the transition structure of the automerization process via the flapping movement of the ring carbons. Thus, the rearrangement of molecular geometries before the Π-bond shifting process broadens the overall reaction path significantly for **20** and **21**, which subsequently hinders the tunneling pathway from the ground vibrational level at cryogenic temperatures for these molecules.

Nevertheless, Kozuch predicted that the HL undergoes facile Π-bond shifting reaction at higher temperatures via thermally activated tunneling process with a half-life of 4×10^{-4} s, at −120°C. As described by the author, at higher temperatures, the planarization of the annulene ring can be achieved easily with the available thermal energy, and once the molecule (**21**) becomes planar, rapid carbon tunneling from the vibrational excited state makes the overall process facile. These results corroborate with the experimental findings of NMR peak broadening at higher temperature of below −120°C and subsequent splitting of ^{13}C signals at −160°C,[34] which is an indication of rapid alternation of the Π-bonds in HL from two localized structures via thermally activated carbon tunneling.

On the other hand, low temperature (−50°C) NMR experiment predicted that the automerization reaction of 1,3,5-tri-tertbutylpentalene (**22a**) occurs rapidly with no traces of double bond localization.[35] Owing to large system size, the detailed SCT calculation is impractical to perform for **22a**. However, Kozuch has tried to take into account the mass effect and conformational flexibility of the three tert-butyl groups in various

imaginative ways while the substitution of ^{1}H with hypothetical super-heavy ^{57}H isotope with mass similar to tert-butyl group was predicted to have minor effect on the reaction kinetics as compared to the unsubstituted PL. Kozuch has pointed out that the displacement of these substituents is negligible throughout the automerization reaction which makes the tunneling rates unaffected by substituents mass. The effect of conformational flexibility of the three tert-butyl groups on the tunneling rates was modeled by performing SCT rate constant calculations on 1,3,5-trimethylpentalene (**22b**). The rate constant for the automerization reaction for **22b** was calculated to be 10^{8} times slower than the PL at 10 K. Therefore, the methyl substitutions significantly affect the tunneling rates and the reason was attributed to the requirement of coupled methyl rotations along with the Π-bond shifting process. As in the preferred conformation of 1,3,5-trimethylpentalene, one C–H bond from each methyl groups aligns itself eclipsed to one of the C–C double bond in the ring and the product also possesses similar conformation. Thus, the methyl substituents must rotate themselves following the Π-bond shifting process; otherwise, the automerization reaction will generate a higher energy conformer of **22b**. It was predicted that the coupled methyl rotations increase both the tunneling mass and width of the barrier which was the reason for the sharp decrease in tunneling rates from **19** to **22b** at low temperatures. The mass effect of the methyl groups in the tert-butyl substituent was modelled more accurately by replacing the ^{1}H of the methyl groups in **22b** by ^{15}H isotope **22c**. Therefore, the increase in effective tunneling mass lowers the computed tunneling rate by 10^{24} times compared to PL, at 10 K, and the author predicted that the automerization of **22c** would not be feasible at such low temperatures. With rise in temperature, the methyl rotations in **22c** become more facile by thermal activation and thermally activated tunneling makes the overall automerization process feasible with a rate constant of $k = 5.3 \times 10^{3}\ s^{-1}$ at 100 K. Also, the author suggested that the 1,3,5-tri-tertbutylpentalene would follow similar kinetics with **22c** and will not automize at cryogenic temperatures whereas thermally activated tunneling enables rapid Π-bond shifting at higher temperature.[33]

4.5c *Carbon tunneling in planar bond shifting of [16]-annulene*: Michel *et al.* have explored the role of heavy-atom tunneling to the Π-bond shifting in another interesting system, namely [16]-annulene (Scheme 7).[36] It has two configurational isomers, **23a** and **23b**, which possess two competitive reaction channels, i.e., planar degenerate bond shifting and conformational change to a more stable isomer. The conformational change was predicted to have a lower barrier than the bond shifting process, making it kinetically feasible pathway, and reaction rate computation without QMT also supports this fact for both the isomers, whereas inclusion of tunneling makes bond shifting faster below 240 K for **23a** and below 140 K for **23b**. Thus, extremely narrow barrier associated with small displacement of the ring carbons facilitates tunneling for bond shifting despite the higher barrier. Nevertheless, both the isomers undergo rapid bond shifting ($t_{1/2}$ = 4.3 and 0.04 s for **23a** and **23b,** respectively, at 80 K) even at cryogenic temperatures because of facile tunneling by 16-ring carbons.

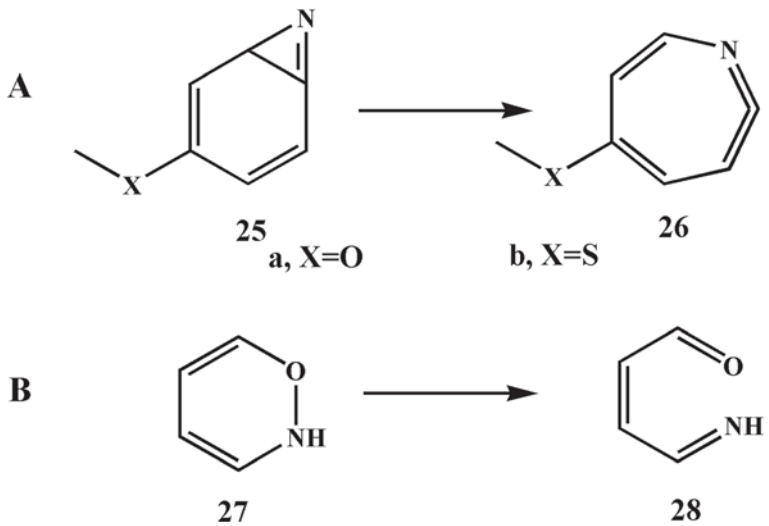

Scheme 8. Electrocyclic ring opening of (A) benzazirines (**25**) and (B) heterocyclic derivative of 1,3-cyclohexadiene (**27**).

4.5d *Tunneling by carbon in the isomerization of cyclopropenyl anions*: Cyclopropenyl anion (**24a**) is the smallest antiaromatic ring system that is known to rearrange through Π-bond shifting process. It comprises a non-planar geometry with C_s symmetry and the ground state is singlet. During the course of automerization reaction, the substituents attached to the ring carbons undergo wide out-of-plane bending motions due to the planarization of the anionic carbon and subsequent deplanarization of one of the double-bonded carbons. Kozuch has analyzed the possibility of tunneling in the automerization reaction of cyclopropenyl anion, and they have also considered its tricyano (**24b**), trimethyl (**24c**), trifluoro (**24d**) and triphenyl (**24e**) derivates to elucidate the effect of substituents in the tunneling process (Scheme 8).[37] They predicted a very facile Π-bond shifting process for **24a** with the rate constant of $k = 2.5 \times 10^6\ s^{-1}$ at cryogenic temperatures, while the calculated rate constants for **24b**, **24c** and **24d** were 2.6×10^{-20}, 4.9 and $8.9 \times 10^{-7}\ s^{-1}$, respectively, which clearly omitted the possibility of automerization for **24b** at cryogenic temperatures. The author attributed such huge difference of 10^{26} times in the calculated rate constants between **24a** and **24b** to the fact that during automerization reaction, the heavy –CN group requires to move through a much wider trajectory to realign itself into the new position of the double bond through the out-of-plane bending motion compared to H in **24a**. On the other hand, although **24c** has a 1.6 kcal/mol lower barrier than **24a**, the automerization process is $\sim 10^5$ times slower than **24a**, owing to the larger mass of methyl than hydrogen. Thus, the author concluded that the rate of the automerization process

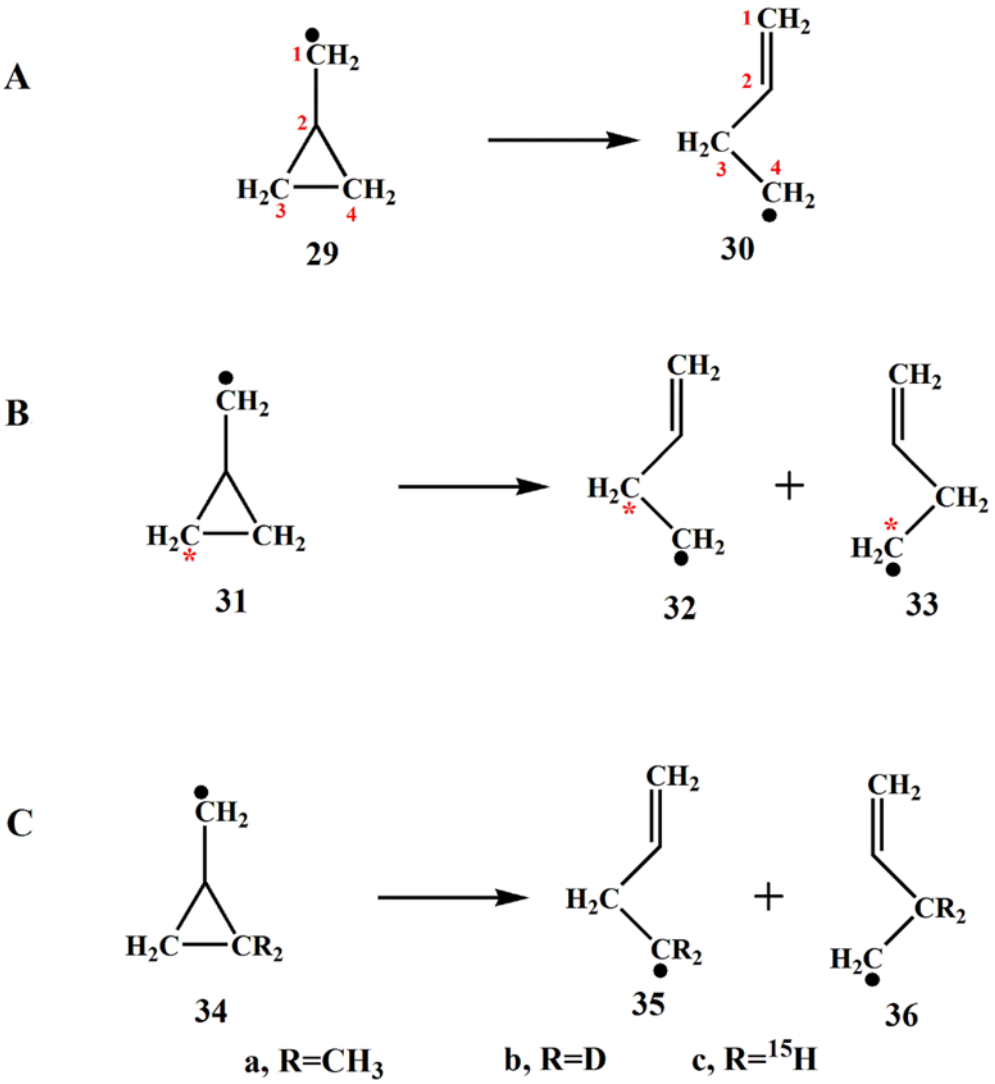

Scheme 9. (A) Ring opening of the cyclopropylcarbinyl radical (**29**) to 3-buten-1-yl radical (**30**), (B) ring opening of the labelled cyclopropylcarbinyl radical (**31**) at one ring carbon (red asterisk) to the **32** and **33** and (C) ring opening of the disubstituted cyclopropylcarbinyl radical (**34**) to corresponding products **35** and **36**.

for the derivatives of cyclopropenyl anion with comparable barrier is strongly governed by the mass and motion of the substituents during the pyramidalization–depyramidalization process. As predicted, the distances between the ring carbons and the substituent ends increase in the following order: cyano (**24b**) > methyl (**24c**) > hydrogen (**24a**) along with the mass of the substituents and hence, the automerization rate follow the inverse order irrespective of the barrier height. Kozuch has also compared the influence of the ring carbons versus the substituent atoms towards the tunneling pathway by calculating their respective KIE ($^{12}C/^{13}C$) for **24c**, and the author found the ring carbons more 'tunneling determining' atoms. In addition, the ground state for triphenylcyclopropyl anion (**24e**) was found to be triplet with equivalent C–C bonds in the ring comprising D_{3h} symmetry; thus, there is no possibility of automerization. The strong Π-acceptor properties of the phenyl substituents favor the aromatic triplet state by delocalizing the electron density out of the cyclopropenyl ring.

4.5e *Heavy-atom tunneling in the ring opening of benzazirines to keteneimines*: Inui *et al.* studied the electrocyclic ring expansion of substituted benzazirines (**25**) to keteneimines (**26**) at cryogenic temperatures in matrix isolation (Scheme 9).[38] They found that the methylthio-substituted benzazirine (**25b**) undergoes the ring opening rearrangement to produce the ketenimine (**26b**) at 10 K even in dark with a rate constant of $k = 1.49 \times 10^{-5}$ s^{-1}. Rising the temperature from 10 to 25 K increases the rate only by a factor of 1.23 which indicates the temperature-independent nature of the rearrangement reaction. The author concluded that the ring opening reaction of **25b** to **26b** occurs by carbon tunneling at low temperatures owing to the occurrence of the reaction at low temperatures and negligible temperature variation of the reaction rate. On the other hand, the methoxy-substituted benzazirine (**25a**) did not undergo the ring expansion rearrangement to **26a** at 10 K. The authors explained the difference in reactivity between the two benzazirine derivatives in terms of the activation barrier and barrier width. The activation barriers were calculated to be 3.4 kcal/mol and 6.9 kcal/mol while the approximate tunneling distances were 0.33 Å and 0.43 Å for **25b** and **25a**, respectively. Therefore, a lower activation barrier and a relatively narrower barrier favor the carbon tunneling mechanism for **25b** at low temperatures.

4.5f *Heavy-atom tunneling in the ring opening of a heterocyclic analog of 1,3-cyclohexadiene*: Hydroxylamine ether (**27**), a heterocyclic analog of 1,3-cyclohexadiene, is a promising candidate where the electrocyclic ring opening might be governed by heavy-atom tunneling (Scheme 9). As a weak N–O bond between the two heteroatoms cleaves upon ring opening, the overall process was predicted to be feasible with a low activation barrier of $\Delta H^{\#} = 6.3$ kcal/mol and exothermic reaction energy of $\Delta H = -35.0$ kcal/mol. Low barrier height along with small displacement of a heavy atom favor the tunneling mechanism for this reaction at cryogenic temperatures. The calculated rate constant for **27→28** was found to be $k = 4.4 \times 10^{4}$ s^{-1} below 30 K and the reaction rates become temperature insensitive. Therefore, the ring opening reaction for **27** was predicted to be very facile because of the heavy-atom tunneling from the lowest vibrational level with a half-life of 10^{-5} s which clearly excludes the possibility of isolation of **27** in reaction conditions. These computational findings of such low lifetime of **27** help to reassign the structure of a product in a reaction.[39] Chen *et al.* initially reported the synthesis and isolation of a dimethyl derivative of **27** from its precursor oxime; however, following the computational prediction and careful reinvestigation of the NMR spectra of the compound, assigned it to 2,4-dimethylhydroxypyrrole not **27**.

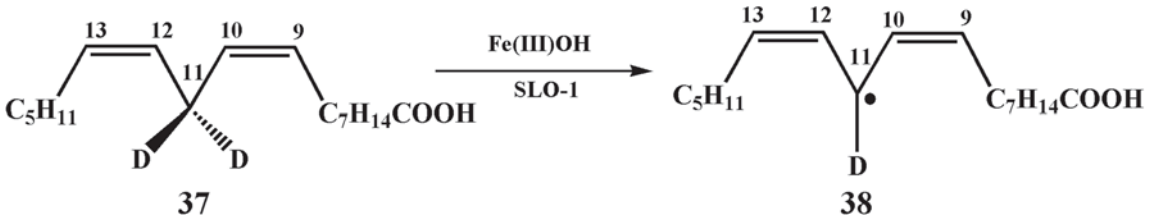

37 38

Scheme 10. Deuterium abstraction from the C-11 position of the linoleic acid-11,11-d_2 (37) catalyzed by SLO-1.

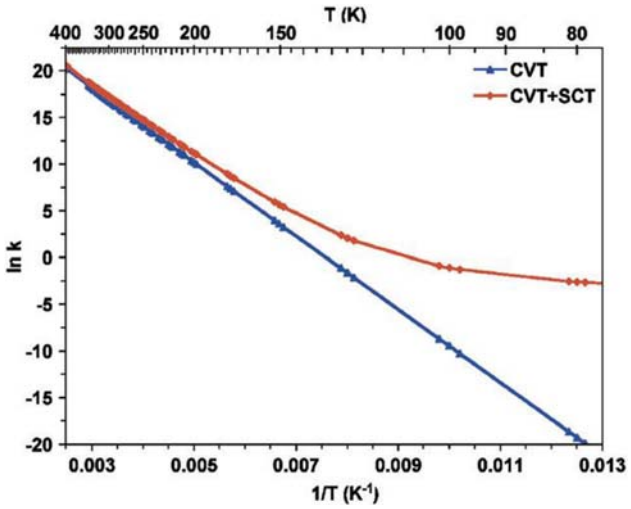

Figure 3. Arrhenius plots of CVT and CVT+SCT rate constants for the **29→30** rearrangement from 80 to 400 K. (Reprinted with permission from ref 18. Copyright © 2008, American Chemical Society.)

4.6 *Computational prediction of carbon tunneling in the ring opening of cyclopropylcarbinyl radical to 3-buten-1-yl radical and its experimental validation by KIE measurement*

Cyclopropylcarbinyl radical (**29**) undergo facile ring opening reaction to form 3-buten-1-yl radical (**30**) at room temperature owing to high strain in the cyclopropane ring (Scheme 10). This rapid reaction is mostly used as a 'radical clock' for measuring the rates of other competitive free radical reactions. In 2008, Datta *et al.* predicted the rapid occurrence of the ring opening reaction of **29** by carbon tunneling at cryogenic temperatures,[18] although the experimental findings over a wide temperature range indicates a thermally activated process for **29→30** transformation with a linear Arrhenius plot. However, a low barrier height (E_a = 7.05 kcal/mol) accompanied by small displacement of the carbon atoms (maximum change in C–C distance is by ∼1 Å) makes it a likely candidate for observing the reaction even at low temperatures by heavy-atom tunneling with a measurable rate constant. Indeed, the SCT calculations confirmed that below 20 K, the reaction occurs by carbon-atom tunneling from the lowest vibrational state with a temperature-independent rate constant of $k = 2.22 \times 10^{-2}$ s^{-1}. Further, SCT calculations initially produce an apparently linear Arrhenius plot at high temperatures which then gets curved at low temperatures and the curvature becomes evident below 150 K (see Figure 3). Even at high temperatures, the SCT-computed Arrhenius parameters show reasonably good agreement with the experimentally measured ones and at 298 K, ∼50% of the reaction occurrs by tunneling. Thus, the authors predicted that the ring opening reaction of **29→30** is rapid at cryogenic temperatures because of carbon-atom tunneling and also, they seek for experimental evidence to validate their computational prediction.

As tunneling rates are very sensitive to the effective mass of the moving particles, Zhang *et al.* have computed various KIEs for the above reaction (**29→30**) as they thought that the KIEs values might provide meaningful insight to the heavy-atom tunneling mechanism at cryogenic temperatures.[40] They reported that the substitution of hydrogen atoms attached with the radical center of **29** by deuterium atoms accelerates the rate of the ring opening, resulting in a large inverse KIE of 0.37 (k_{CH2}/k_{CD2} = 0.37) at cryogenic temperatures. This result is contradictory to the normal convention that tunneling rates decrease with increasing mass of the participating atoms producing a large normal KIE, while isotopic substitutions at the other carbon centers follow the usual trend and SCT calculations computed a large KIE (k_{CH2}/k_{CD2} = 6.47) for the ring carbon (C4) of **29-d$_2$** that opens up to the radical center in **30**.

To explain these unusual findings, a careful examination of the animation of the transition vector for the ring opening step of **29→30** was carried out. It was found that the radical center (C1) and the atoms attached to it show negligible movement throughout the ring opening process and the C4 ring carbon undergoes maximum displacement along the reaction coordinate due to which the isotopic substitutions at C4 result in large normal KIE. Accordingly, it is expected that isotopic substitution of the hydrogens by deuteriums at the C1 center should not have any effect on the tunneling rates with a KIE of ∼1.00.

However, due to structural changes ongoing from **29** to **30**, the vibrational frequencies for the torsion about the C1–C2 bond and the pyramidalization of the radical C1 center increases subsequently from **29** to the transition state connecting them to **30** and hence, the zero-point energies (ZPEs). As vibrational frequencies are inversely proportional to the mass of the atoms, these increase in frequencies ongoing from **29** to **30** is much smaller for C^1D_2 than C^1H_2. Thus, the effective barrier height of the ring opening reaction for C^1D_2 is lower by 0.24 kcal/mol compared to the C^1H_2 owing to smaller increase in ZPEs. A lower reaction barrier leads to a higher tunneling rates for C^1D_2 and hence, an inverse KIE is observed at the radical center (C1) of **29** for the ring opening reaction. Instanton theory also provides similar KIEs as computed by SCT calculations for the **29→30** reaction except for the C4

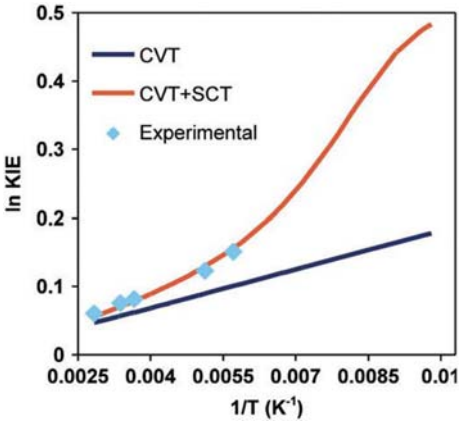

Figure 4. Arrhenius plots of the CVT, CVT+SCT and experimental ^{13}C KIE data for the ring opening of **31** to **32** and **33** from 100 to 353 K. (Reprinted with permission from ref 19. Copyright © 2010, American Chemical Society).

ring carbon. Instanton theory predicts that the isotopic substitution at this carbon (C4) yields CH_2/CD_2 KIE of 13.35 at 20 K while it was calculated to be 6.47 at SCT level. The actual value of KIE at C4 can only be verified by experimental measurements.

To validate the computational predictions of Zhang *et al.*, in 2010, Gonzalez-James *et al.* have measured the ^{13}C KIEs for the ring opening reaction of cyclopropylcarbinyl radical (Scheme 10).[19] They reported strikingly large KIEs for the ring carbon that become radical center in **30**. Isotopic substitution at one of the ring carbons (C3/C4) makes the ring opening reaction asymmetric and the relative product ratio (**32**:**33**) is governed by tunneling as stretching of the C-C bond forming the radical center in **30** is the primary motion along the reaction coordinate. It was found that the C-C bond cleavage is more favorable when the radical is generated on the $^{12}CH_2$ moiety rather than the $^{13}CH_2$ group because of grater mass of ^{13}C. Measuring the distribution of ^{13}C at C3 and C4 position of **31** provides the intramolecular KIEs. Gonzalez-James *et al.* generated the cyclopropylcarbinyl radical from the bromo-methylcyclopropane by free-radical chain condition and then the resulting product radicals, **32** and **33**, were trapped by tributyltin hydride ($(C_4H_9)_3SnH$) to give 1-butene. The distribution of ^{13}C at different positions (C3 or C4) of 1-butene was measured by ^{13}C NMR spectroscopy. The authors plotted the measured KIEs against 1/T along with two other plots of KIEs computed at CVT level for the thermally activated process and at CVT + SCT level for the tunneling reaction (see Figure 4). For over-the-barrier process, a linear Arrhenius plot of KIE was observed (see the blue line in Figure 4), whereas for tunneling-mediated reactions, the KIEs are expected to be greater than the KIEs of the thermally activated process because of mass effects, and the effect of tunneling on KIEs will be prominent at lower temperatures producing a curved Arrhenius plot. As can be seen from Figure 4, the Arrhenius plot of KIE at CVT + SCT level shows similar characteristics, indicating a tunneling mechanism for this reaction. Interestingly, the experimentally measured KIEs match closely with the tunneling corrected KIE values and the Arrhenius plot of experimentally measured KIEs shows similar non-linear behavior over the studied temperature range of 173–253 K. Therefore, readily observable curvature in the Arrhenius plot of experimentally measured KIE for the ring opening reaction of **31** act as a strong experimental signature of heavy-atom tunneling in this reaction.

Inspired by the experimental evidence of tunneling in the ring opening reaction of **31**, Zhang *et al.* have studied the effect of germinal methyl group substitution at one of the ring carbons on the rate of tunneling and how the bond breaking is affected by this substitution (Scheme 10).[41] At room temperature or above, 2,2-dimethylcyclopropylcarbinyl radical (**34a**) undergo ring opening reaction producing **35a** as the major product with a product ratio of **35a**:**36a** = 6.5 :1.[42,43] This is obvious because the formation of tertiary radical as in **35a** is thermodynamically more favorable compared to the formation of primary radical as in **36a**. Also, greater stability of the tertiary radical leads to lower ring opening barrier for **34a**→**35a** making it kinetically favorable compared to **34a**→**36a**.

However, the authors were curious to see the outcomes when the ring opening reaction of **34a** was carried out at cryogenic temperatures as at these temperatures, there will be no thermal energy available and the reaction will be governed by tunneling. Hence, the authors expected that the formation of **36a** might be favorable at lower temperatures because heavier methyl groups might retard the tunneling rates for the C–C bond cleavage of **34a**→**35a** transformation. However, SCT calculations predicted a different picture, it was found that the formation of **35a** was favored compared to **36a** by a factor of 7.76×10^5. Also, the rate of ring opening of **34a**→**35a** was predicted to be 10^4 times higher than the unsubstituted analog (**29**→**30**). Hence, these findings clearly indicate that the mass effect of the geminal methyl groups is not the only factor that affects the tunneling rates. They have explained these unusual finding on the basis of other two factors; barrier height and barrier width.

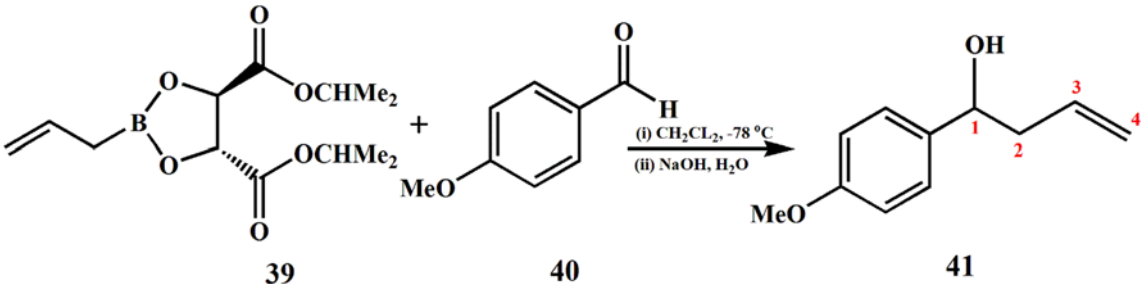

Scheme 11. Allylboration reaction of p-anisaldehyde (**40**) with Roush's reagent.

The higher exothermicity of the **34a**→**35a** reaction lowers the activation barrier for the **35a** formation by 1.7 kcal/mol compared to the formation of **36a**. According to Hammond's postulate, more exothermic reactions possess earlier transition states than the less exothermic ones and the early transition structure is coupled with narrower barrier. Indeed, SCT calculations predicted a narrower barrier for **35a** and the respective barrier widths for the formation of **35a** and **36a** were calculated to be 0.54 Å and 0.83 Å. Therefore, a lower activation barrier along with a narrower barrier facilitates the tunneling mechanism more for **35a** despite of heavier tunneling mass resulting in a calculated product ratio of $\sim 10^6$:1, favoring the formation of **35a** over **36a** at cryogenic temperatures.

4.7 *Experimental evidence of carbon tunneling in the H-abstraction reaction from linoleic acid-11,11-d_2 by soybean lipoxygenase-1*

Soybean lipoxygenase 1 (SLO-1) can activate selective C–H bonds of hydrocarbon molecules. Hydrogen abstraction catalyzed by SLO-1 from the C-11 position of the linoleic acid produces large primary H/D KIE of about 80 and hence, the reaction undoubtably occurs by hydrogen-atom tunneling at room temperature (Scheme 11). To investigate the effect of backbone atoms on the H-tunneling step, Meyer and Klinman have measured the ^{13}C KIEs at several carbons of linoleic acid-11,11-d_2 (**37**) for the deuterium abstraction reaction catalyzed by the enzyme SLO-1. Interestingly, substantial ^{13}C KIEs have been observed at positions 9–13 of the linoleic acid-11,11-d_2 for the

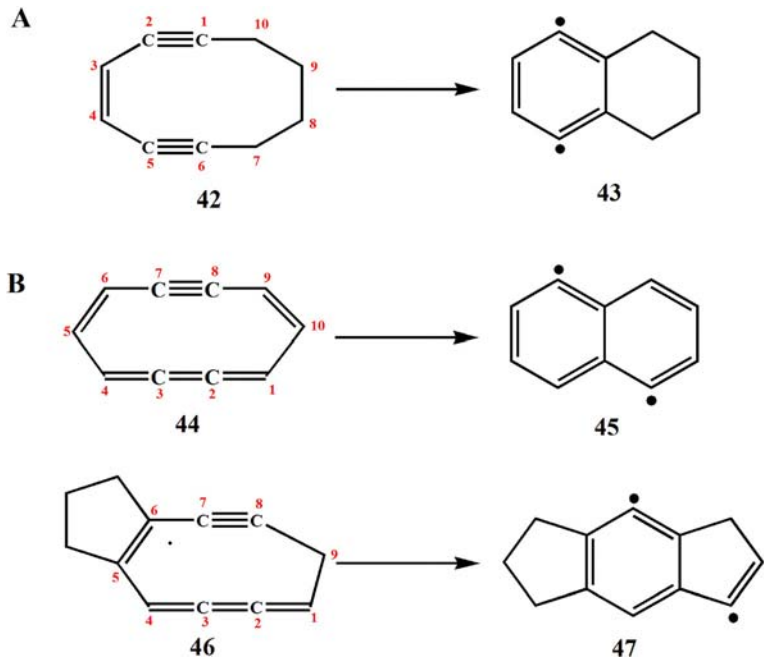

Scheme 12. (A) Bergman cyclization of cyclic 10-membered enediyne **42** and (B) Myers–Saito cyclization of cyclic 10-membered and 9-membered enyne-cumulenes **44** and **46.**

deuterium abstraction reaction and the C-11 center possesses the largest $^{12}C/^{13}C$ KIE value of 1.045 ± 0.029. In order to determine the upper limit of KIE values, the authors have calculated the equilibrium isotope effect (EIEs) using 2,5-heptadiene as the model substrate to represent the linoleic acid. It was found that the ^{13}C EIEs for the 2,5-heptadiene-4,4-d_2 to be 1.015–1.019 for the deuterium abstraction reaction. Therefore, the authors attributed the observation of strikingly large ^{13}C KIEs at the C-11 of **37** to the coupled motion of C-11 during the D-abstraction reaction by tunneling pathway.[1]

4.8 *Experimental evidence of carbon tunneling in the allylboration of p-anisaldehyde by Roush's reagent*

Vetticatt *et al.* have measured the intermolecular ^{13}C KIEs for the allylboration reaction of aldehyde (**40**) by Roush's reagent (**39**) at −78°C (Scheme 12).[44] It was found that the carbonyl carbon of **40** (C1) and the C2 and C4 centers of **39** produce substantial KIEs as all of them undergo changes in σ-bonding pattern in the rate-determining step. The largest value of $^{12}C/^{13}C$ KIE was observed for carbonyl carbon of **40** and it was measured to be 1.052 ± 0.005 at −78°C. They have reported that the predicted KIEs based on conventional TST with inclusion of solvent effects by polarized continuum model (PCM) are way off than the measured KIEs. However, incorporation of tunneling and recrossing effects by canonical variational TST (CVT) and small-curvature tunneling (SCT) methods yield KIEs that show excellent agreement with measured KIEs. At −78°C, the calculated $^{12}C/^{13}C$ KIEs for the C1 carbon were found to be 1.041 and 1.052 at TST and CVT+SCT level, respectively. Therefore, the agreement between the SCT calculated KIE values to the experimentally measured ones, indicate the decisive influence of heavy-atom tunneling in this reaction. Also, the rate of the reaction shows 1.36-fold enhancement due to tunneling at reaction temperature. Nevertheless, the authors concluded that the effects of heavy-atom tunneling in everyday organic reactions are mostly hidden from chemists as there is no theory or independent way to know the rate of the reaction in the absence of tunneling. Only the KIE measurement provides valuable insight on the heavy-atom tunneling mechanism.

4.9 *Heavy-atom tunneling in cyclization reactions*

4.9a *Heavy-atom tunneling in the Bergman cyclization of cyclic enediyne*: Greer *et al.* investigated the role of heavy-atom tunneling in the Bergman cyclization of cyclic (3Z)-cyclodec-3-en-1,5-diyne (**42**) (Scheme 13).[21] The cyclization reaction of the enediyne, **42**, follow a linear Arrhenius plot in the temperature range of 310–343 K with an activation barrier (E_a) of 23.8 kcal/mol and the computed barrier height was 24.2 kcal/mol. As the barrier for the cyclization reaction was found to be both high and wide, the authors proposed that thermally activated tunneling will take place. Detailed SCT calculations support the fact and it was found that the tunneling occurs from the top of the barrier within 1–2 kcal/mol of the reaction barrier. As the tunneling is mostly confined within a specific energy range to the top of barrier, the effective barrier width also becomes narrow at this region and the authors calculated the width of the barrier for **42**→**43** to be 0.2 Å, where the contribution of tunneling to the reaction rate is most significant.

The reaction rate constant calculations for the **42**→**43** transformation show that 40–60% of the reaction is occurring by carbon-atom tunneling from the excited vibrational level in the temperature range of 200–343 K. The Arrhenius plot was found to be linear over this temperature range because the

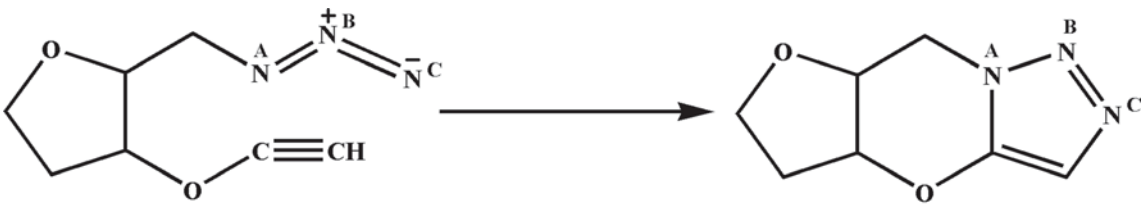

48 **49**

a, A, B, C=^{14}N **b, A=^{15}N; B, C=^{14}N**

Scheme 13. Intramolecular Huisgen reaction of **48.**

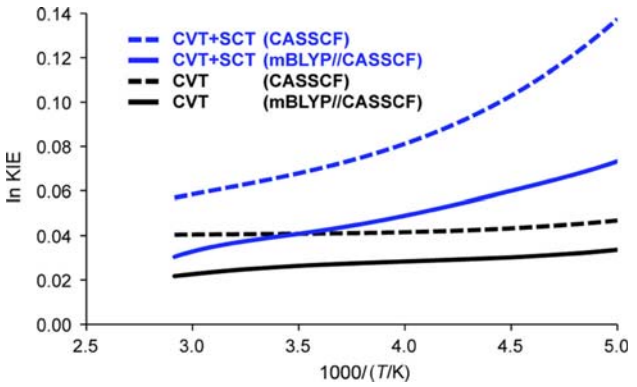

Figure 5. Arrhenius plots of the CVT and CVT+SCT KIE data for the **42**→**43** cyclization reaction. (Reprinted with permission from ref 21. Copyright © 2013, American Chemical Society).

widening of the barrier at lower energies restricts the atom tunneling from the ground vibrational level. As reaction rate measurements cannot provide the exact contribution of tunneling in a particular reaction, its experimental detection often gets difficult without any characteristics proof.

For this reason, the authors have studied the effects of tunneling on the $^{12}C/^{13}C$ KIEs such that occurrence of heavy-atom tunneling in this cyclization reaction might be detected experimentally by ^{13}C KIE measurements. It was found that the tunneling has substantial effect on the KIE and a curved Arrhenius plot (see the blue lines in Figure 5) of KIE is observed in the temperature range of 200–343 K. The curvature arises due to the increase of tunneling mass upon ^{13}C substitution at the C1 position of **42** lowers the tunneling probability and, hence, the reaction rate. At 250 K, KIEs with and without tunneling corrections were calculated to be 1.049 and 1.028, respectively. Thus, the authors proposed that the distinguishable curvature in the Arrhenius plot of KIE for **42**→**43** transformation can be verified experimentally.

4.9b *Tunneling by carbon in the Myers−Saito cyclization of cyclic enyne-cumulene*: Karmakar and Datta have reported the evidence of heavy-atom tunneling in the Myers-Saito cyclization reaction of cyclic 10-membered and 9-membered enyne-cumulene systems namely, 1,6-didehydro[10]annulene (**44**) and derivative of neocarzinostatin (**46**) (Scheme 13).[17] It was found that the effects of tunneling (∼100 K) are most prominent at low temperatures resulting an 5–10 times rate enhancement for both the reactions. The rate constant calculations reveal that the tunneling corrected rate ($k_{CVT+SCT}$) for **44** is 1.32 times greater than the classical rate (k_{CVT}) resulting in $k_{CVT+SCT}$ = 3.26×10^{-4} s^{-1} at 222 K. The half-lives ($t_{1/2}$) were predicted to be 45 min (without tunneling) and 35 min (with tunneling) at 222 K for **44**, whereas the experimentally measured $t_{1/2}$ was 21–31 min, therefore, close proximity of the experimentally observed half-life with the SCT calculated one indicates contribution of heavy-atom tunneling in such cyclization reaction. Furthermore, calculations of primary (1°), secondary (2°) and both (1°+2°) ^{13}C KIE for **44**, predicted that the CVT+SCT KIEs are always larger than the CVT KIEs. At 222 K, the CVT+SCT computed (1°+2°) ^{13}C KIE was found to be 1.134 which is ∼9% larger than its classical value. Also, heavy-atom tunneling results in appreciable curvature in the Arrhenius plot of ^{13}C KIE at ambient conditions.

4.10 *Heavy-atom tunneling in the intramolecular Huisgen reactions*

Karmakar and Datta investigated the role of heavy-atom tunneling in the intermolecular and intramolecular Huisgen reactions.[45] It was found that the intramolecular cycloaddition reaction (**48**→**49**) has a significant contribution of nitrogen tunneling on reaction kinetics at ambient conditions (Scheme 14). At 298 K, an enhancement of ∼35% in reaction rate was predicted due to heavy-atom tunneling despite the large activation barrier of 22.5 kcal/mol and the SCT rate was computed to be $k = 7.35 \times 10^{-7}$ s^{-1}. A narrow barrier of ∼2.4 Å in **48** facilitates tunneling for this intramolecular reaction. The $^{14}N/^{15}N$ KIEs were calculated to be 1.04 (with tunneling) and 1.01 (without tunneling), at 298 K, irrespective of the nitrogen substitution center. Thus, it was proposed that designing conformationally restricted intramolecular click reactions based on the cyclooctyne rings might have strong heavy-atom tunneling contributions.

4.11 *Excited state carbon tunneling in the Zimmerman di-π-methane rearrangement*

Li *et al.* predicted that the electronically excited-state carbon tunneling plays crucial role in the di-π-methane (DPM) rearrangement of polycyclic molecules, namely dibenzobarrelene (DBB, **48a**), benzobarrelene (**48b**) and barrelene (**48c**) (Scheme 14).[46] The DPM rearrangement occur in triplet (T_1) potential energy surface in two consecutive steps, (**48**→**49** and **49**→**50**) involving radical intermediates and the overall change in the reacting carbon distances are quite small (Δd = 0.8–0.9 Å). For DBB, **48a**, the first step is the

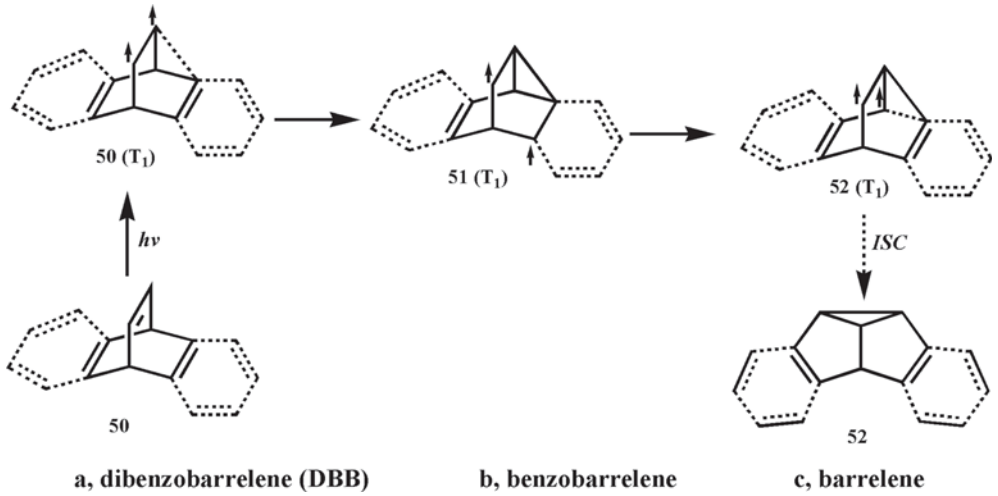

Scheme 14. Di-π-methane rearrangement of dibenzobarrelene (**50a**), benzobarrelene (**50b**) and barrelene (**50c**) to corresponding products **52a/52b/52c**.

rate determining step (**48a→49a**) with an energy barrier of 10.8 kcal/mol and it was found that the carbon tunneling contributes significantly to the computed reaction rates and ^{13}C KIEs even at 200–300 K. It was predicted that the tunneling enhances the reaction rate by 33–63% in the temperature range of 200–300 K and below 160 K, the Arrhenius plot of reaction rates shows strong curvature. At 200 K, the SCT rate constant for **48a→50a** was calculated to be 4.78×10^2 s^{-1}. Also, substitution by ^{13}C at the reacting carbons lowers the tunneling probability remarkably and the computed $^{12}C/^{13}C$ KIEs were found to be much higher when tunneling by carbon was incorporated (1.165 vs 1.079 at 200 K), suggesting vibrationally activated tunneling. The other two systems, **48b** and **48c**, also show similar characteristics. Therefore, the first reported example of excited-state carbon tunneling could be tested experimentally by natural abundance ^{13}C NMR method and reaction rate measurements.

4.12 *Tunneling by carbon in the flipping reaction of formaldehyde on Cu (110) surface*

Lin *et al.* have investigated the flipping dynamics of formaldehyde (CH_2O) between its two mirror-reflected states on the Cu (110) surface by low-temperature scanning tunneling microscopy. DFT computations along with STM experiments indicate the presence of three different adsorption configurations of formaldehyde namely, η^1, η^2 and η^3 (see Figure 6a), among which the η^3 configuration possess a very low flipping barrier of ~20 meV. By monitoring the flipping dynamics of CH_2O in real times, the authors observed that the reaction rate is independent of temperature below 10 K. Thus, the authors concluded that the flipping reaction of the η^3 configuration of CH_2O occurs by tunneling and the very small barrier for this reaction facilitates the carbon-tunneling from the ground vibrational state despite significant motion of the carbon atom (~1 Å).[47]

4.13 *Effect of heavy-atom tunneling for 'fleeting' molecules*

Hoffmann, Schleyer, and Schaefer have coined the term 'fleeting'[48] for those hypothetical molecules which are required to be only at local minima on a PES. Their existence has been predicted based on computational studies of their vibrational frequencies; however, they possess a very small rearrangement barrier which makes them kinetically labile at ambient conditions. Nevertheless, at cryogenic temperatures, their isolation might be feasible because of insufficient thermal energy to overcome the barrier. However, Kozuch predicted that facile heavy-atom tunneling from the ground vibrational level makes their isolation impossible even at cryogenic temperatures.

A bridged tetrahedryl–tetrahedrane (see Figure 6b) is a highly strained molecule which possess the shortest theoretically predicted C–C bond. Because of high strain in the tetrahedrane moieties, it is prone to undergo rearrangement to a carbene via ring contraction with an activation enthalpy ($\Delta H^{\#}$) of 6.7 kcal/mol. SCT calculations by Kozuch predicted that even at 0 K, the rearrangement of F.1 to carbene is very rapid because of carbon tunneling with a temperature-independent rate constant of $k = 1.7 \times 10^2$ s^{-1}. Thus, the

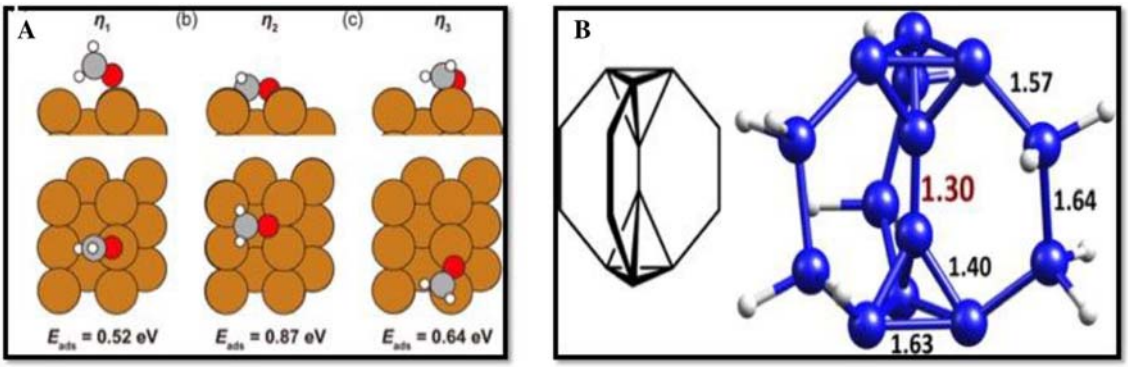

Figure 6. (A) The adsorption configurations (η^1, η^2 and η^3) of formaldehyde (CH_2O) on the Cu (110) surface and their corresponding adsorption energies. (Reprinted with permission from ref 47. Copyright © 2019, American Chemical Society). (B) Structure of bridged tetrahedryl-tetrahedrane (Reprinted with permission from ref 49. Copyright © 2014, American Chemical Society).

author concluded that such a small lifespan of ($t_{1/2}$ = 4 ms at 0 K) will hinder its isolation under any conditions.[49]

Another interesting system is $C(CH_3)_5^+$, a pentacoordinated carbocation, which was predicted to have fleeting existence. It has two low energy degradation pathways, among which one produces a tertiary carbocation while the other one yields ethane and tert-butyl carbocation. Calculations without inclusion of QMT predicted that the reaction will take several millennia to occur at 20 K, while the computed half-lives for the disappearance of $C(CH_3)_5^+$ by heavy-atom tunneling was found to be only 10^{-5}–10^{-6} s^{-1}, below 20 K. Therefore, the author suggested that it is highly important to check the 'tunneling stability' of the molecules close to 0 K before its computational prediction to be fleeting.[50]

5. Conclusion

After 86 years of the prediction that 'all atoms heavier than helium behave classically,' it is unquestionable that the significance of heavy-atom tunneling in common organic reactions is as important as H-tunneling. Several experimental and theoretical studies have indicated that the effect of heavy-atom tunneling is not only limited to cryogenic temperatures, it contributes considerably to the reaction rate even at room temperatures. Sometimes experimental detection of heavy-atom tunneling is difficult because of the limited experimental techniques. However, computational studies always provide meaningful insight, which even direct experimentalist to carry out further experiments to test computational prediction. We hope that in the coming years, there will be many more examples of reactions with significant heavy-atom tunneling contribution. We believe that in future, experimental techniques will be more sophisticated and computational studies will be more accurate which will eventually instigate the detection of heavy-atom tunneling in common reactions. Furthermore, modulation of different reaction parameters, especially barrier width, might result in tunneling controlled product over conventional thermodynamic and kinetic control for reactions involving significant heavy atom motions. In the next few years, the phenomenon of heavy-atom tunneling in common organic reactions will be more established and its effect will be ubiquitous.

Acknowledgement

AD thanks SERB and DST for partial funding.

References

1. Truhlar D G 2010 Tunneling in enzymatic and nonenzymatic hydrogen transfer reactions *J. Phys. Org. Chem.* **23** 660
2. Platz M S, Moss R A and Jones M 2006 Preface *Rev. React. Intermed. Chem.* **1** 472
3. Nagel Z D and Klinman J P 2006 Tunneling and dynamics in enzymatic hydride transfer *Chem. Rev.* **106** 3095
4. Ley D, Gerbig D and Schreiner P R 2012 Tunnelling control of chemical reactions – the organic chemist's perspective *Org. Biomol. Chem.* **10** 3781
5. Kohen A 2003 Kinetic isotope effects as probes for hydrogen tunneling, coupled motion and dynamics contributions to enzyme catalysis *Prog. React. Kinet. Mech.* **28** 119
6. Karmakar S and Datta A 2014 Tunneling assists the 1,2-hydrogen shift in N-heterocyclic carbenes *Angew. Chemie - Int. Ed.* **53** 9587

7. Bell R P 1933 The application of quantum mechanics to chemical kinetics *Proc. R. Soc. A Math. Phys. Eng. Sci.* **139** 466
8. Buchwalter S L and Closs G L 1975 An electron spin resonance study of matrix isolated 1,3-cyclopentadiyl, a localized 1,3-carbon biradical *J. Am. Chem. Soc.* **97** 3857
9. Whitman D W and Carpenter B K 1982 Limits on the activation parameters for automerization of cyclobutadiene-1,2-d2 *J. Am. Chem. Soc.* **104** 6473
10. Carpenter B K 1983 Heavy-atom tunneling as the dominant pathway in a solution-phase reaction? bond shift in antiaromatic annulenes *J. Am. Chem. Soc.* **105** 1700
11. Doubleday C, Armas R, Walker D, Cosgriff C V and Greer E M 2017 Heavy-atom tunneling calculations in thirteen organic reactions: tunneling contributions are substantial, and Bell's formula closely approximates multidimensional tunneling at $\geq$ 250 K *Angew. Chemie Int. Ed.* **56** 13099
12. Borden W T 2016 Reactions that involve tunneling by carbon and the role that calculations have played in their study *Wiley Interdiscip. Rev. Comput. Mol. Sci.* **6** 20
13. Meisner J and Kästner J 2016 Atom tunneling in chemistry *Angew. Chemie Int. Ed.* **55** 5400
14. Buchwalter S L and Closs G L 1979 Electron spin resonance and CIDNP studies on 1, 3-cyclopentadiyls. A localized 1, 3 carbon biradical system with a triplet ground state. Tunneling in carbon-carbon bond formation *J. Am. Chem. Soc.* **101** 4688
15. Sponsler M B, Jain R, Corns F D and Dougherty D A 1989 Matrix-isolation decay kinetics of triplet cyclobutanediyls. Observation of both arrhenius behavior and heavy-atom tunneling in C—C bond-forming reactions *J. Am. Chem. Soc.* **111** 2240
16. Gerbig D, Ley D and Schreiner P R 2011 Light- and heavy-atom tunneling in rearrangement reactions of cyclopropylcarbenes *Org. Lett.* **13** 3526
17. Karmakar S and Datta A 2016 Role of heavy atom tunneling in myers-saito cyclization of cyclic enyne-cumulene systems *J. Phys. Chem. B* **120** 945
18. Datta A, Hrovat D A and Borden W T 2008 Calculations predict rapid tunneling by carbon from the vibrational ground state in the ring opening of cyclopropylcarbinyl radical at cryogenic temperatures *J. Am. Chem. Soc.* **130** 6684
19. Gonzalez-James O M, Zhang X, Datta A, Hrovat D A, Borden W T and Singleton D A 2010 Experimental evidence for heavy-atom tunneling in the ring-opening of cyclopropylcarbinyl radical from intramolecular 12C/13C kinetic isotope effects *J. Am. Chem. Soc.* **132** 12548
20. Zhang X, Hrovat D A and Borden W T 2010 Calculations predict that carbon tunneling allows the degenerate cope rearrangement of semibullvalene to occur rapidly at cryogenic temperatures *Org. Lett.* **12** 2798
21. Greer E M, Cosgriff C V and Doubleday C 2013 Computational evidence for heavy-atom tunneling in the Bergman cyclization of a 10-membered-ring enediyne *J. Am. Chem. Soc.* **135** 10194
22. Kozuch S 2014 The reactivity game: theoretical predictions for heavy atom tunneling in adamantyl and related carbenes *Phys. Chem. Chem. Phys*. https://doi.org/10.1039/c4cp00115j
23. Moss R A, Sauers R R, Sheridan R S, Tian J and Zuev P S 2004 Carbon tunneling in the ring expansion of noradamantylchlorocarbene *J. Am. Chem. Soc.* **126** 10196
24. Fernandez-Ramos A, Ellingson B A, Garrett B C and Truhlar D G 2007 Variational transition state theory with multidimensional tunneling In *Reviews in computational chemistry* **23** 125
25. Bell R P 1980 In *The Tunnel Effect in Chemistry* (Chapman & Hall) p. 77
26. Greer E M, Kwon K, Greer A and Doubleday C 2016 Thermally activated tunneling in organic reactions *Tetrahedron* **72** 7357
27. Guthrie J P, Platz M S, Moss R A and Jones M 2007 Review of Reactive Intermediate Chemistry. In *Wiley Interscience* p. 3–46
28. Ertelt M, Hrovat D A, Borden W T and Sander W 2014 Heavy-atom tunneling in the ring opening of a strained cyclopropene at very low temperatures *Chem. A Eur. J.* **20** 4713
29. Sulzbach H M, Platz M S, Schaefer H F and Hadad C M 1997 Hydrogen migration vs carbon migration in dialkylcarbenes. A study of the preferred product in the carbene rearrangements of ethylmethylcarbene, cyclobutylidene, 2-norbornylidene, and 2-bicyclo[2.1.1]hexylidene *J. Am. Chem. Soc.* **119** 5682
30. Zuev P S, Sheridan R S, Albu T V, Truhlar D G, Hrovat D A and Borden W T 2003 Carbon tunneling from a single quantum state. *Science (80-.).* **299** 867
31. Cheng A K, Anet F A L, Mioduski J and Meinwald J 1974 Determination of the fluxional barrier in semibullvalene by proton and carbon-13 nuclear magnetic resonance spectroscopy *J. Am. Chem. Soc.* **96** 2887
32. Schleif T, Mieres-Perez J, Henkel S, Ertelt M, Borden W T and Sander W 2017 The cope rearrangement of 1,5-dimethylsemibullvalene-2(4)-d1: experimental evidence for heavy-atom tunneling *Angew. Chemie - Int. Ed.* **56** 10746
33. Kozuch S 2014 Heavy atom tunneling in the automerization of pentalene and other antiaromatic systems *RSC Adv.* **4** 21650
34. Vogel E, Königshofen H, Wassen J, Mullen K and Oth J F M 1974 A heptalene synthesis from 1,6-methano[10]annulene; evidence for a fast π-bond shift *Angew. Chemie Int. Ed. English* **13** 732
35. Hafner K and Süss H U 1973 1,3,5-Tri-tert-butylpentalene. a stabilized planar 8π-electron system *Angew. Chemie Int. Ed. English* **12** 575
36. Michel C S, Lampkin P P, Shezaf J Z, Moll J F and Castro C, Karney W 2019 Tunneling by 16 carbons: planar bond shifting in [16]annulene *J. Am. Chem. Soc.* **141** 5286
37. Kozuch S 2015 Cyclopropenyl anions: carbon tunneling or diradical formation? A contest between Jahn-Teller and Hund *J. Chem. Theory Comput.* **11** 3089
38. Inui H, Sawada K, Oishi S, Ushida K and McMahon J 2013 Aryl nitrene rearrangements: Spectroscopic observation of a benzazirine and its ring expansion to a

ketenimine by heavy-atom tunneling *J. Am. Chem. Soc.* **135** 10246
39. Chen B, Scott M E, Adams B A, Hrovat D A, Borden W T and Lautens M 2014 Computational and 13C investigations of the diazadienes and oxazadienes formed via the rearrangement of methylenecyclopropyl hydrazones and oximes *Org. Lett.* **16** 3930
40. Zhang X, Datta A, Hrovat D A and Borden W T 2009 Calculations predict a large inverse H/D kinetic isotope effect on the rate of tunneling in the ring opening of cyclopropylcarbinyl radical. *J. Am. Chem. Soc.* **131** 16002
41. Zhang X, Hrovat D A, Datta A and Borden W T 2011 Effects of geminal methyl groups on the tunnelling rates in the ring opening of cyclopropylcarbinyl radical at cryogenic temperature *Org. Biomol. Chem.* **9** 3142
42. Newcomb M, Glenn A G and Williams W G 1989 Rate constants and arrhenius functions for rearrangements of the 2,2-dimethyl-3-butenyl and (2,2-dimethylcyclopropyl)methyl radicals. *J. Org. Chem.* **54** 2675
43. Beckwith A L J and Bowry V W 1989 Kinetics and regioselectivity of ring opening of substituted cyclopropylmethyl radicals. *J. Org. Chem.* **54** 2681
44. Vetticatt M J and Singleton D A 2012 Isotope effects and heavy-atom tunneling in the Roush allylboration of aldehydes *Org. Lett.* **14** 2370
45. Karmakar S and Datta A 2015 Metal free azide-alkyne click reaction: role of substituents and heavy atom tunneling *J. Phys. Chem. B* **119** 11540
46. Li X, Liao T and Chung L W 2017 Computational prediction of excited-state carbon tunneling in the two steps of triplet zimmerman di-π-methane rearrangement *J. Am. Chem. Soc.* **139** 16438
47. Lin C, Durant E, Persson M, Rossi M and Kumagai T 2019 Real-space observation of quantum tunneling by a carbon atom: flipping reaction of formaldehyde on Cu(110) *J. Phys. Chem. Lett.* **10** 645
48. Hoffmann R, Schleyer P V R and Schaefer H F 2008 Predicting molecules - more realism, please! *Angew. Chemie - Int. Ed.* **47** 7164
49. Kozuch S 2014 A quantum mechanical Jack in the box: Rapid rearrangement of a tetrahedryl-tetrahedrane via heavy atom tunneling *Org. Lett.* **16** 4102
50. Kozuch S 2015 On the tunneling instability of a hypercoordinated carbocation *Phys. Chem. Chem. Phys.* **17** 16688